Appl. Phys. B (2013) 111:7–14
DOI 10.1007/s00340-012-5298-9

Applied Physics B
Lasers and Optics

Double pulse quasi-collinear high harmonic generation scheme as a tool for X-ray laser plasma gain probing

Sameh Daboussi · Sophie Kazamias · Kevin Cassou · Olivier Guilbaud · Moana Pittman · Olivier Delmas · Olivier Neveu · Brigitte Cros · Gilles Maynard · David Ros

Received: 22 June 2012 / Accepted: 9 November 2012 / Published online: 22 December 2012

Abstract We have investigated high harmonic generation in an argon gas cell driven by two femtosecond laser pulses separated by a variable delay ranging from 500 fs to 100 ps. Experiments were performed at the LASERIX IR-EUV facility using an amplified 10 Hz CPA Ti:Sapphire laser system on a beamline delivering 50 fs pulses at 800 nm with energy up to 25 mJ. In the case of a non-zero time delay we studied the optimal conditions for equilibrated double pulse generation despite perturbation of the generating medium induced by the first pulse. We showed how high harmonic double pulse generation varies with the gas pressure, the excitation energy, the delay and the relative polarization between the two laser pulses.

1 Introduction

High order harmonic generation (HHG) is a nonlinear coherent interaction process between atoms and a driving laser field which produces ultra-short coherent radiation reaching the soft X-ray region [1–3]. HHG has been used as a powerful table top tool for a number of applications such as holography [4] and nonlinear optics [5].

One of the emerging and very promising applications of HHG is the seeding of plasma-based soft X-ray laser (SXRL) [6, 7] and free electron lasers [8]. Traditionally, these systems use to work respectively in the amplification of spontaneous emission (ASE) regime or self-amplification of spontaneous emission (SASE) regime. This presents some limitations in terms of the extreme UV (EUV) beam optical properties [9, 10]. Strong enhancement of beam collimation, spatial coherence and temporal coherence has been demonstrated in plasma-based SXRL by seeding proper EUV beam. This opens the way to sources combining the high output energy of SXRL source with the spatial and temporal coherence of the HHG source [11, 12]. It is important to point out that seeding requires not only well-characterized and optimized harmonics but also high enough energy in order to dominate the spontaneous emission signal.

We investigate in this paper the possibility to generate a seed pulse with a double temporal structure with variable delay in the picosecond range. This waveform would be attractive for different EUV-EUV pump-probe experiment but also to study more deeply the plasma-based SXRL seeding temporal aspects like gain build up and recovery time [13] or medium polarization evolution [14].

The first harmonic pulse would act as a pump by triggering the gain depletion and the second one as a probe of the residual gain and the polarization behavior of the amplifying plasma. A popular scheme to obtain efficient EUV amplification in a plasma is the transient collisional excitation (TCE) in which the pumping of population inversion in pre-existing ions is induced by a short laser pulse via electron collisional excitations, leading to high gain value at short wavelength. For this type of experiment,

S. Daboussi (✉) · S. Kazamias · K. Cassou · O. Guilbaud · O. Neveu · B. Cros · G. Maynard · D. Ros
LPGP, CNRS, UMR 8578, Univ. Paris-Sud, Bat 210, Campus d'Orsay, 91405 Orsay Cedex, France
e-mail: sameh.daboussi@u-psud.fr

S. Daboussi · S. Kazamias · K. Cassou · O. Guilbaud · M. Pittman · O. Delmas · O. Neveu · D. Ros
LASERIX, CLUPS- LUMAT, Univ. Paris-Sud, CNRS FR 2764, Campus d'Orsay, 91405 Orsay Cedex, France

O. Delmas
Amplitude Technologies, 2-4 rue du bois chaland-CE, 91029 Evry, France

the relevant temporal range of interest ranges from 500 fs to 10 ps, as gain duration inferred from ASE pulse duration measured with streak cameras [15] or cross correlation [16] techniques are of the order of a few picoseconds. We will therefore concentrate our study on double pulse seed with delay covering this temporal range.

2 Position of the problem

To our knowledge due to fundamental and technical issues, HHG pumped by two close following short pulses in the picosecond range has not been studied extensively except for zero delay. First of all, the pump energy level required to generate high energy per harmonic pulse is rather high (5–10 mJ minimum for argon gas) and not often available on the kilohertz laser installations dedicated to HHG studies and applications. Secondly, it is well known that HHG is a multi-photon process closely linked with laser field ionization of gases, so that no efficient harmonic generation can really take place without a small amount of ionization [17]. Conversely, ionization causes electronic dispersion in the generating gas which is detrimental for phase-matching [18]. Efficient harmonic generation in a pre-ionized medium that has already generated a harmonic pulse is thus a non-trivial issue. This was observed in the early 2000s by the CEA-Saclay group when they performed HHG interferometry [19]; in this case the HHG beam generated by the second pulse in the same gas target was so perturbed that they preferred to generate two different HHG sources originating from two different gas targets. Significant results were then obtained using such a device for EUV plasma interferometry [20] at the price of a complex optical system. The advantage of our configuration is that alignments are considerably simplified as compared to double target systems, because the two-pulse EUV lies in the same beam leading therefore to simplifier arrangement for SXRL experiments seeding. The present work aims at studying the problem of double pulse HHG from the same medium, in terms of its temporal response, the influence of phase-matching optimization with respect to pumping energy and gas pressure in the case of efficient loose focusing geometry [21].

3 Quasi collinear generation process

A key issue for the double harmonic pulse generation and optimization is the possibility to discriminate between two EUV pulses generated with a time delay in the picosecond range for pump-probe experiments. It is indeed important to fully characterize behavior of the second pulse independently with respect of the first one, in terms of total energy, spectrum and transverse profile. Extreme UV streak cameras could hardly reach such temporal resolution but the complex working conditions they require, together with their small dynamic range make them hard to use. We made the choice to use a slightly non-collinear double pulse conversion configuration. For this, the two laser excitation pulses were shaped in a Mach–Zehnder type interferometer with variable delay and are non-collinearly recombined at focus, in the gas cell. This was done with as small angle as possible so as to make them spatially overlapping such as if they were collinear. As will be shown later, the interaction volumes of both pulses overlap at 90 %. Because of the low harmonic divergence, the two harmonic beams generated by each of the pulses can then be distinguished on far field detectors after a few meters of propagation thanks to the non-collinear geometry. As an illustration Fig. 1 shows the footprints of HHG beams generated by each isolated beam and by their combination at a delay of 10 ps.

Non-collinear techniques have already been studied for several applications in the case of zero delay between the two pulses, for example in order to increase the yield of various low-order wave mixing processes [22, 23], to separate generated EUV from excitation IR beam by generating a HHG beam in the middle direction resulting from the coherent mixing of the two intensities, ultra high-order wave mixing with cross angle about 14 mrad [24]. In some conditions, when the cross angle is more important (30 mrad), non-collinear high harmonic generation can be used as an out coupling method for cavity assisted EUV generation [25]. Theoretical interpretations of the results obtained for zero delay have been proposed in terms of infrared field enhancement and modified phase-matching conditions as early as 2002 [23], and more recently the two color experiment from [24] was interpreted in terms of perturbation theory. Our experiment and its interpretation are radically different in the sense that the two consecutive pulses generating the double temporal structure are not interfering in the gas medium when generating HHG. To our knowledge, our experimental setup with both controllable infrared energy and temporal delay in the picosecond range is a new approach for HHG based applications.

4 Experimental setup

The experimental investigation was carried out at LASERIX, a high-power laser facility fully dedicated to the development and applications of SXRL beams in the range of 7–30 nm [26]. The IR source used in our experiment is based on a low energy sampling from the amplified Ti:Sapphire laser system that provides 50 fs duration pulses centered at a wavelength of 800 nm. Due to pulse air

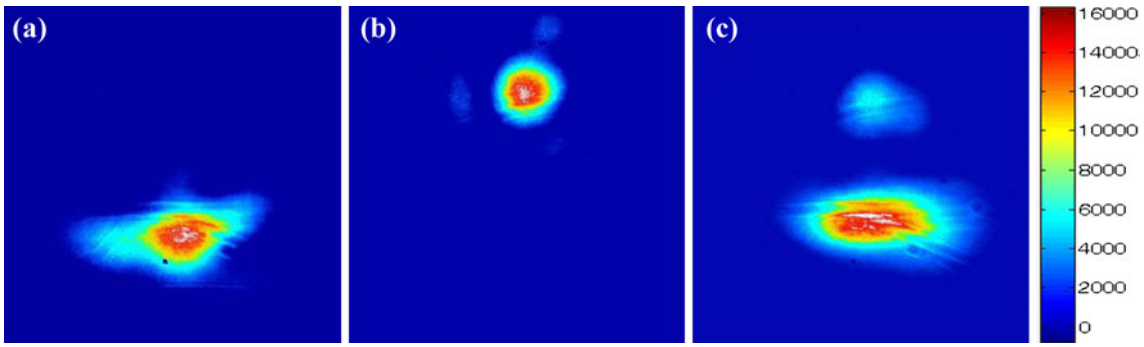

Fig. 1 **a**, **b** Footprints of HHG beams generated in 15 mbar of argon by each isolated IR beam of 1.5×10^{14} W/cm^2. **c** Footprints of HHG beams generated in 15 mbar of argon by both the first (*lower trace*) and the second (*upper trace*) IR beams for a delay of 10 ps. Footprints measured 3 m away from the HHG source. Transverse separation is about 1 mm corresponding to an angular separation of about 1mrad between the 2 beams

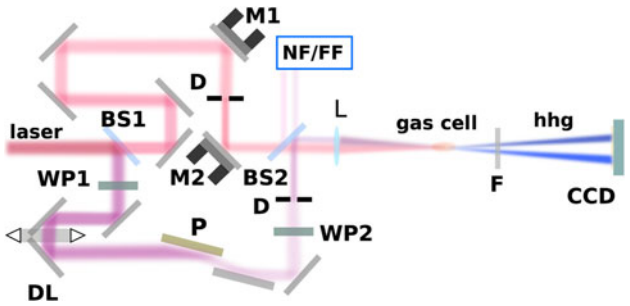

Fig. 2 Experimental setup for quasi-collinear HHG: BS, beamspliter 50/50; WP1, half wave plates; P, Brewster Polarizer; NF, real time near field control; FF, real time far field control; D, iris diaphragm; L, lens f = 1100 mm and F, Al 0.2 μm thick filter. The polarization of the reflected pulse is controlled using the wave plate WP2. Reflected energy sent on the cell is adjusted with WP1+P

compression, the maximum energy dedicated to HHG is limited to 25 mJ at a repetition rate of 10 Hz. The schematic of our setup for quasi-collinear HHG is shown on Fig. 2. The incoming laser pulse is injected into a Mach–Zehnder type system equipped with an adjustable length arm in order to control the delay (−100 ps, +100 ps) between the reflected and the transmitted pulses. The temporal resolution of the system was 6 fs limited by the motorized translation stage accuracy. The polarization of the two beams could be set parallel or perpendicular to each other. A polarizer associated with a zero order half wave plate was installed in the path of the reflected beam in order to adjust its energy. Variable apertures were placed on both the reflected and the transmitted beams to adjust intensities and focusing geometries [21].

The two beams are recombined with a 50/50 thin beam splitter with a small transverse separation of about 1 mm and then focused into the gas cell with an f1100 mm lens with a small angle. The recombination angle which is of the order of 1 mrad was chosen in order that, considering their own divergence which is also about 1 mrad for each HHG pulse, the two EUV beams do not overlap on the detector situated 3 m away from the gas cell. The footprints of the two generated EUV beams were recorded 3 m further from the source on a backlighted EUV CCD camera (Fig. 1). The harmonic spectrum is then analyzed by a transmission-grating spectrometer coupled to a backlighted EUV CCD camera placed at a similar distance from the source. The generation medium is a 10 mm long gas cell which center is placed on the focal plane of the IR beams. The beam waist has been measured to be $w_0 = 80$ μm (half-width at $1/e^2$) for both beams. The 1 mrad angle between them leads to a maximum spot separation of 5 μm into the generating medium, one order of magnitude smaller than the waist value. The transmitted laser light and high harmonic orders higher than 47 were blocked by an aluminum filter (0.2 μm thickness). After energy optimization in argon for HHG signal separately for each pulse, only 10 mJ of the 25 mJ available energy was used in our configuration. The estimated energy per harmonic beam is 70 pJ using the CCD and filter calibration and referring to previous EUV calibrated photodiode [27] data obtained in similar conditions. In those conditions a precise laser alignment is crucial to achieve precise superposition of the beams in the focal region. A real time control of near and far fields showed that the two focal spots still spatially superimposed throughout the cell when varying the delay.

5 Temporal delay effect

5.1 Experimental investigation

After HHG optimization of each of the two individual beams, EUV generation using both of them simultaneously was studied. For a null delay between the two quasi-collinear pulses, a clear on-axis signal was observed similar to observation reported in already mentioned works [23] and

[25] giving confidence in correct superposition and timing of both IR pulses. The influence of the delay was then analyzed for equivalent generation conditions on both arms (15 mbar of argon, same IR intensity about 1.5×10^{14} W/cm^2). Figure 3 shows the delay scan from 500 fs to 100 ps of the normalized integrated signals of the two HHG beams recorded with the EUV-CCD camera. These curves were obtained by the ratio between the measurements of the total integrated EUV signal generated by the first (resp. the second) IR beam in the double and single pulse configurations. Each IR pulse was first individually optimized in order to obtain two equivalent EUV signals on the CCD footprint (with 16 bits dynamic). These signals were used as references for the two pulse configuration. Each measurement was averaged over five laser shots and the experiment was repeated over several days with real time spatial control of the superposition of the two focal spots as shown on Fig. 1 (NF-FF). The represented error bars are attributed to HHG signal fluctuations due to shot to shot variations of laser energy. The slow drift of the laser pointing mainly due to delay line adjustment were checked and corrected before each acquisition.

As expected, the first pulse is not affected by the presence of the second one. The ratio slightly higher than one is not significant since it represents the ratio over two integrated signals measured with an interval of few tens of minutes. For the pulse arriving later, the signal ratio is approximately half maximum value for any kind of delay in the range studied. This indicates that HHG phase-matching for the second pulse is presumably perturbed by the ionization due to the first one. Moreover, this alteration of the generation conditions does not seem to depend on the delay, even for values as long as 100 ps. The same behavior was observed for parallel and perpendicular pulses polarization.

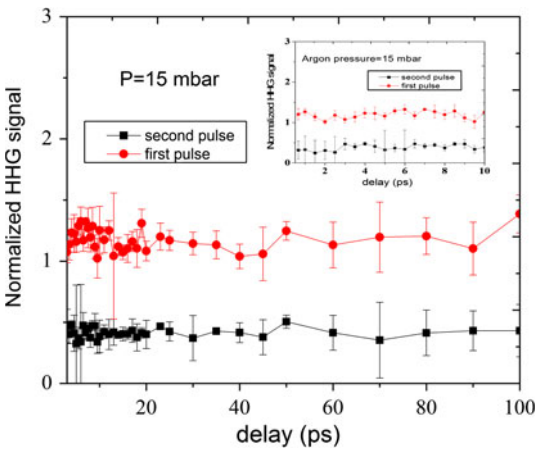

Fig. 3 Measured HHG signal generated by the first pulse (*circle*) and by the second pulse (*square*) as a function of the delay in 15 mbar of argon. These measurements correspond to encircled energy recorded on the CCD normalized with respect to the corresponding single HHG beam

5.2 Theoretical estimations for plasma recombination characteristic time

This independence with delay of harmonic generation condition for the second pulse has been investigated theoretically. As mentioned above, the optical field of the first intense pulse ionizes the medium. Using the Ammosov–Delone–Krainov (ADK) ionization rate (τ) [28], a maximum of 5 % of the argon atoms are expected to be ionized in our experimental conditions for a 25 mbar argon pressure and a maximum intensity of 1.5×10^{14} W/cm^2.

Calculations have been performed using a zero dimension (0D) optical field ionization (OFI) code predicting the energy distribution of electrons coupled to a collisional radiative model [29–31]. Temperature predicted for heavy particle (atoms and ions) is close to the room temperature whereas electrons reach a 0.5 eV temperature immediately after the first pulse interaction. In that case, neither hydrodynamic expansion which is estimated to be about 0.15 μm during 100 ps nor excitation by collisions have time to play a significant role. Besides, for this low temperature, the energy exchange between electrons and heavy particles is dominated by ion-electron collisions with a characteristic time of 1 μs leading to a negligible cooling of the electron gas of 0.01 % in 100 ps. Moreover the recombination rates are also small. In this context, the three body recombination mechanism is dominant. However, the direct recombination to the fundamental state has a characteristic time of the order of 1 ms and only recombination to highly excited states can then have a significant rate. These excited neutral atoms decay slowly to the fundamental state, with a characteristic time of 2 ns. Moreover, they are more rapidly ionized by the optical field of the second pulse than neutral atoms in the ground state. From the harmonic generation point of view the excited neutral species behave as ionized species.

In summary, these theoretical estimations show that the plasma effective recombination time is of the order of a few nanoseconds. Once perturbed by the first pulse, the generating medium does not significantly evolve on tens of picosecond timescales. The behavior remains stable during more than 100 ps, so for the following parts, the time delay between the two pulses will be arbitrarily set at 10 ps.

6 Spectra discussion

The recorded HHG emission spectra generated by the two IR pulses in 15 mbar of argon are displayed in Fig. 4. The upper curves show the estimated spatially integrated

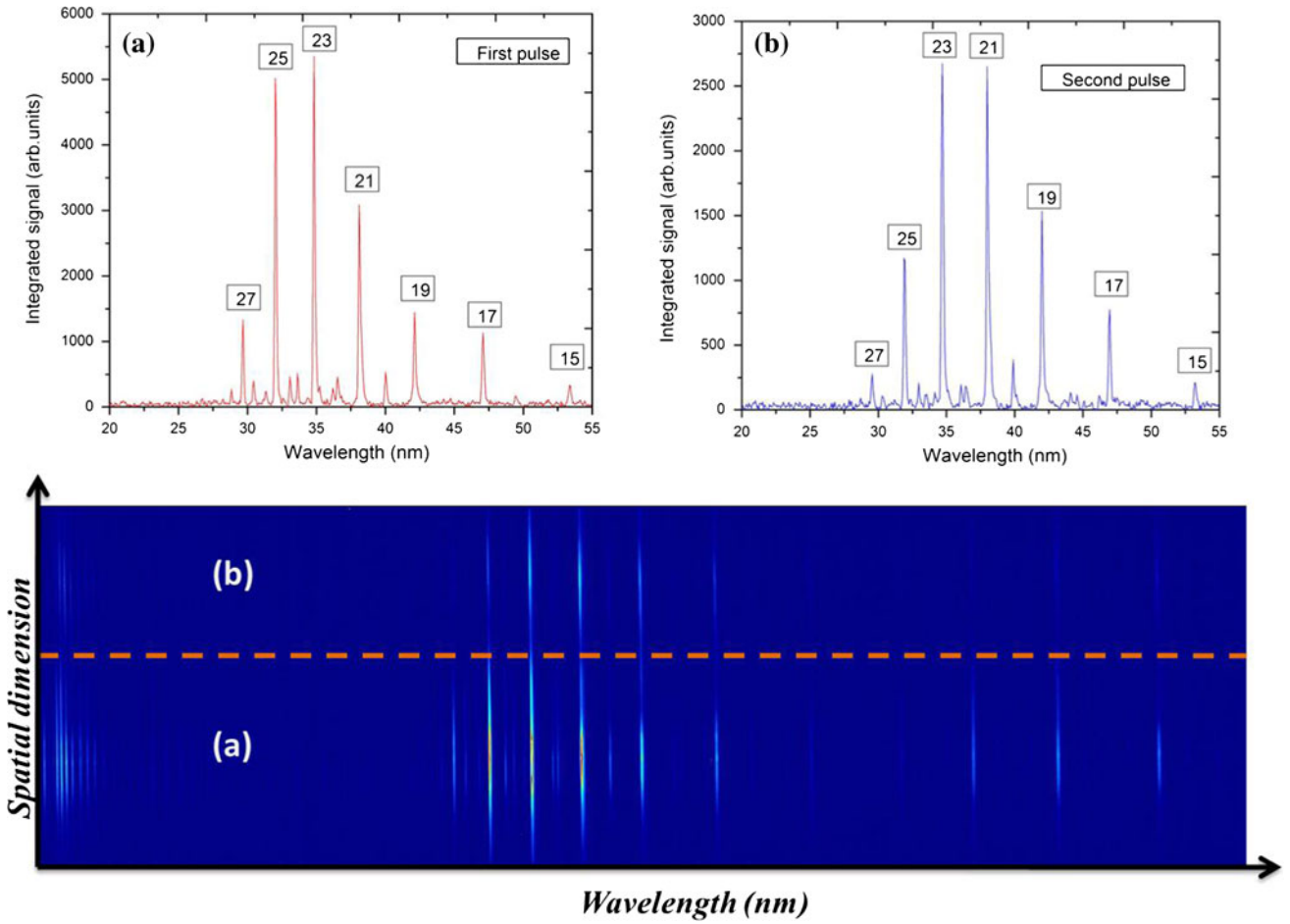

Fig. 4 Measured harmonic spectra generated in 15 mbar of argon from: **a** the first IR beam and **b** the second IR beam. The delay is fixed to 10 ps. For both spectra we observe the same harmonics from 15 to 27

photon flux per harmonic order with respect to wavelength. The lower pictures shows the spectra recorded in one image for 2 mJ of IR energy in both pulses measured for a diaphragm aperture of 11 mm diameter on both beams and the time delay was arbitrarily set at 10 ps.

As shown in Fig. 4, in both spectra we observe the same peaks occurring at odd multiples of the driving laser frequency from 15th to 27th (53.33–29.62 nm) corresponding to the same cutoff. Neither spectral shift nor widening is observed for the second HHG pulse.

The spectral shift compared to the central wavelength can occur for the second pulse if during the generation, a temporal variation of the atomic phase gradient ($\alpha\frac{\delta I}{\delta t}$), the atomic dispersion (δk_{at}) or the electronic dispersion (δk_{elec}) [32] is induced by the first pulse, with $\alpha = 2 \times 10^{-14}$ cm^2/W for the first quantum path and $\alpha = 22 \times 10^{-14}$ cm^2/W for the second quantum path.

After interaction with the first pulse, the generation conditions for the second one are certainly not the same as for the first. The electronic and atomic dispersions are modified, but no modification of their temporal derivative can take place since the ionization rate in the medium does not depend on the time since we consider no coherent effect between the two laser pulses can appear at such timescale. We can also remark that the harmonics from both spectra are spatially well confined (low divergence 1 mrad), thus a dominant contribution from the short trajectory may be assumed. This can explain why there is no spectral modification in the spectrum of the second pulse despite the ionization in the medium before generation.

We couldn't measure the duration of the two HHG pulses because we do not have the appropriate setup. But we can conclude from the spectrum of the second pulse that no temporal change has occurred since no spectral broadening is observed.

Future work will aim to inject the 25th harmonic into SXRL plasma amplifiers pumped by intense optical laser pulses on a solid titanium target (32.6 nm line of neon-like titanium). So, there is keen interest for the injection experience to generate the same harmonics with a temporal double pulse structure to probe the SXRL plasma gain.

7 Phase matching optimization

For the following study, the temporal delay was set at 10 ps and we optimized the infrared energy and the gas pressure in order to balance the intensity of the two HHG beams. Maximum HHG signal was obtained independently for each excitation beam with comparable pulse peak intensities of 1.5×10^{14} W/cm^2 resulting from 2 mJ of the 50 fs IR pulses with an aperture size at near field of 11 mm. The waists of the driving beams at focus were w_0 = 80 µm (half-width at 1/e^2). The same studies were done in the case of parallel and perpendicular pumping polarization and for the same working conditions, the same results were observed.

7.1 Infrared energy effect

For the curve presented in Fig. 5, we varied the IR pump energy of the first pulse from 0 to 2 mJ with fixed energy for the second pulse of 1.5 mJ. This figure displays the evolution of both signals generated by the first (square) and the second (circles) pumping pulses.

As predicted by the classical atomic model of HHG [17], the EUV signal generated by the first pulse increases with IR energy. On the other hand, for 1 mJ of the first pumping energy the two curves intersect, so the EUV signal of both beams is balanced, at about 40 pJ/shot for each EUV pulse. For a relatively low energy of the first pulse (below 0.8 mJ), the EUV signal generated by the second pulse decreases slowly but remains around 70 pJ/shot. Then, it falls sharply when the IR energy of the first pulse increases up to 1.5 mJ. Finally, this EUV signal turns off above 1.5 mJ of the first pumping energies.

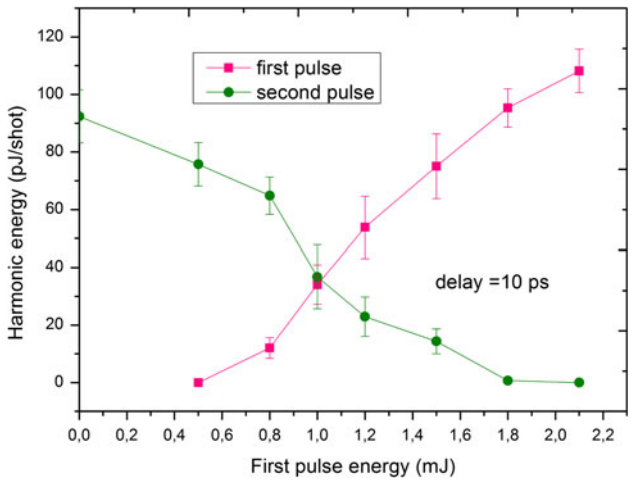

Fig. 5 Variation of the harmonic signal generated by: the first beam (*squares*) and the second beam (*circles*) by function of IR energy of the first pulse. Energy of the second pulse remains constant around 1.5 mJ. The argon pressure was 15 mbar and the time delay between two pulses was fixed at 10 ps

We can interpret the decrease of the second pulse EUV energy as a function of the first pumping energy by the increase of the ionization rate in the generating medium.

The effect of the ionization rate on the signal evolution of the second pulse has been investigated using a one dimensional (1D) time-dependent code of HHG described in detail in [33]. Using this code, we have studied the temporal evolution of the ionization rate in the generating medium after interaction with only the first pulse, and then after interaction with the two pumping pulses. The temporal evolution of the coherence length, which is the characteristic length of the phase matching, was also studied.

We consider the case of two consecutive equivalent pumping pulses with the same intensity of about I = 1.2×10^{14} W/cm^2 for 1.5 mJ. After interaction of the first pulse with the generating medium, the ionization rate passes from 0 to 2.5 %, corresponding to a coherence length evolution from 6.7 to 3.5 mm. These values are not negligible and allow achieving a good HHG signal level. This can explain the high signal level of the second EUV pulse when the first pumping pulse energies are low.

As we introduced earlier, it is reasonable to assume that the medium does not change between the first and the second pumping pulse. The second pulse interacts with an already ionized medium, the ionization rate increases from 2.5 to 4.9 %. Therefore, the coherence length decreases up to 2.5 mm. This latter value, which is much smaller than the medium length (10 mm), leads to a dramatically reduced HHG signal.

Considering the phase matching, for a fixed pressure, high ionization rate is not favorable for efficient HHG generation [33] because the atomic positive dispersion is no more able to compensate for the electronic dispersion induced by ionization. So to ensure that the second pulse is efficiently generated, it is necessary to limit ionization rate of the medium after interaction with the first IR beam. At a given pressure, it is then necessary to use less IR energy for the first beam than in the second one. A simple solution in our case is to use a 40/60 for the recombining beams splitter instead of a classical 50/50 one.

7.2 Pressure effect

Figure 6 presents on a semi logarithmic scale the signal measured for the two HHG beams as a function of the gas pressure, the excitation beams being balanced. The laser intensity for each pulse in that experiment was estimated around 1.75×10^{14} W/cm^2, corresponding to a high ionization rate of the gas, and the time delay between the two pulses was arbitrarily set at 10 ps.

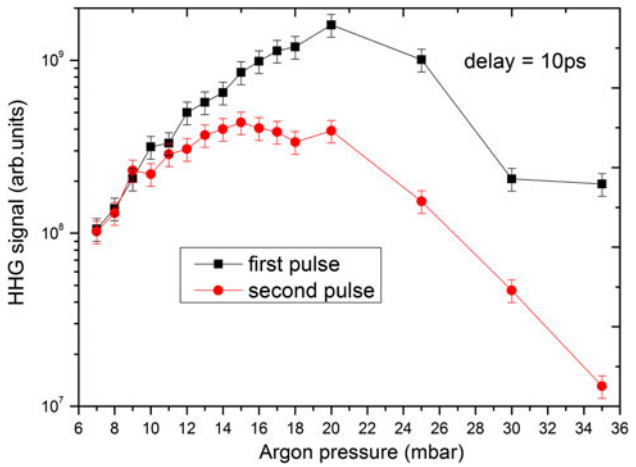

Fig. 6 Variation of the harmonic signal generated by: the first beam (*circles*) and the second beam (*squares*) as a function of argon pressure. The laser intensity at the focus for each infrared beam was estimated around 1.75×10^{14} W/cm^2 and the time delay between two pulses was fixed at 10 ps

The two EUV pulses are optimized for a pressure of 20 mbar; in this case the EUV signal generated by the first pulse was one order of magnitude higher than the second one. For higher pressure, both signals decrease as the pressure continues to increase.

In the case of lower pressures, the two EUV beams tend to be balanced. For this case the signal generated by the first pulse is 20 times lower than the optimum value. So in order to balance the two EUV pulses in the case of high ionization we have to decreases the pressure.

This can be explained in terms of HHG phase matching at high ionization level, typically (τ higher than 4 %). In that case [33], the phase mismatch is almost linear with both ionization and pressure. In the presence of strong intensity, it is necessary to work at low gas pressure in order to balance the energy of the two EUV beams. The same study conducted at low intensity, shawn no strong effect of the pressure in that case. To conclude, the pressure plays an important role on the balance of the two pulses only in the case of high ionization.

8 Conclusion

In conclusion, generation of two quasi-collinear EUV pulses arising from the same high-order harmonic medium and separated by delay of 500 fs up to 100 ps has been investigated. A versatile experimental setup has been used to generate two infrared pulses with controlled delay, angle, energy and polarization. The first pulse perturbs the medium by ionization, changing the generation conditions for the following pulse. When the two pulses are not temporally superimposed, we experimentally checked that the time delay does not play any role in the generation of the double pulse up to 100 ps, which is consistent with theoretical recombination time scale. For a fixed delay, phase matching optimization was carried out to balance the EUV energy in the two pulses. The IR energy of the first pulse was found to be the key parameter, and gas pressure plays only a role in the case of high intensity since we worked in the loose focusing configuration. Due to the very high spatial overlap of the two generating IR beams throughout the gas cell, results obtained here can reasonably be extrapolated to perfectly collinear pulses. Besides, we confirmed that the observed behavior does not depend on the relative polarization states, parallel or crossed, of the two IR generating pulses. Moreover, the spectra of the two EUV pulses remain identical. These three properties are of great interest for plasma-based soft X-ray laser seeding experiments aiming at probing the gain and polarization dynamics of the amplifier stage. This type of study gives also insight into the physics of very high repetition rate harmonics, above 1 GHz.

Acknowledgments We acknowledge the support of the ANR project "Jeunes chercheuses et jeunes chercheurs ASOURIX ANR-09-JCJC-0056".

References

1. M. Lewenstein, Ph. Balcou, M.Y. Ivanov, A. L'Huillier, P.B. Corkum, Phys. Rev. A. **49**, 2117 (1994)
2. C.-G. Wahlstrom, J. Larsson, A. Persson, T. Starczewski, S. Svanberg, P. Salieres, Ph. Balcou, A. L'Huillier, Phys. Rev. A **48**, 4709 (1993)
3. C.G. Durfee, A.R. Rundquist, S. Backus, C. Herne, M.M. Murnane, H.C. Kapteyn, Phys. Rev. Lett **83**, 2187 (1997)
4. A.S. Morlens, J. Gautier, G. Rey, P. Zeitoun, J.P. Caumes, M. Kos-Rosset, H. Merdji, S. Kazamias, K. Cassou, M. Fajardo, Opt. Lett. **31**, 3095–3097 (2006)
5. N.A. Papadogiannis, L.A.A. Nikolopoulos, D. Charalambidis, G.D. Tzakiris, P. Tzallas, K. Witte, Phys. Rev. Lett **90**, 133902 (2003)
6. P. Zeitoun, G. Faivre, S. Sebban, T. Mocek, A. Hallou, M. Fajardo, D. Aubert, P. Balcou, F. Burgy, D. Douillet, S. Kazamias, G. de Lacheze-Murel, T. Lefrou, S. le Pape, P. Mercere, H. Merdji, A.S. Morelens, J.P. Rousseau, C. Valentin, Nature (London) **431**, 426 (2004)
7. Y. Wang, E. Granados, F. Pedaci, D. Alessi, B.M. Luther, M. Berrill, J.J. Rocca, Nat. Photon. **2**, 94 (2008)
8. G. Lambert, T. Hara, D. Garzella, T. Tanikawa, M. Labat, B. Carre, H. Kitamura, T. Shintake, M. Bougeard, S. Inoue, Y. Tanaka, P. Salieres, H. Merdji, O. Chubar, O. Gobert, K. Tahara, M.E. Couprie, Nat. Phys. **4**, 296 (2008)
9. O. Guilbaud, A. Klisnick, D. Joyeux, D. Benredjem, K. Cassou, S. Kazamias, D. Ros, D. Phalippou, G. Jamelot, C. Moller, Eur. Phys. J. D. **40**, 125 (2006)
10. O. Guilbaud, A. Klisnick, K. Cassou, S. Kazamias, D. Ros, G. Jamelot, D. Joyeux, D. Phalippou, Eur. Phys. Lett. 74, 823 (2006)
11. J.P. Goddet, S. Sebban, J. Gautier, Ph. Zeitoun, C. Valentin, F. Tissandier, T. Marchenko, G. Lambert et al., Opt. Lett. **34**, 2438 (2009)

12. M. Berrill, D. Alessi, Y. Wang, S.R. Domingue, D.H. Martz, B.M. Luther, Y. Liu, J.J. Rocca, Opt. Lett. **35**, 2317 (2010)
13. T. Mocek, S. Sebban, G. Maynard, Ph. Zeitoun, G. Faivre, A. Hallou, M. Fajardo, S. Kazamias, B. Cros, D. Aubert et al., Phys. Rev. Lett. **95**, 173902 (2005)
14. E. Oliva, Ph. Zeitoun, M. Fajardo, G. Lambert, D. Ros, S. Sebban, P. Velarde, Phys. Rev. A **84**, 13811 (2011)
15. A. Klisnick, J. Kubal, D. Ros, R. Smith, G. Jamelot, C. Chenais-Popovics, R. Keenan, S.J. Topping, C.L.S. Lewis, F. Strati, G.J. Tallents, D. Neely, R. Clarke, J. Collier, A.G. MacPhee, F. Bortolotto, P.V. Nickles, K.A. Janulewicz, Phys. Rev. A. **65**, 033810 (2002)
16. T. Mocek, S. Sebban, I. Bettaibi, L.M. Upcraft, P. Balcou, P. Breger, P. Zeitoun, S. Lepape, D. Ros, A. Klisnick, A. Carillon, G. Jamelot, B. Rus, J.-F. Wyart, Appl. Phys. B **78**, 939–944 (2004)
17. P.B. Corkum, Phys. Rev. Lett. **71**, 1994 (1993)
18. S. Kazamias, D. Douillet, F. Weihe, C. Valentin, A. Rousse, S. Sebban, G. Grillon, F. Auge, D. Hulin, Ph. Balcou, Phys. Rev. Lett. **90**, 193901 (2003)
19. H. Merdji, J.-F. Hergott, M. Kovacev, E. Priori, P. Salieres, B. Carre, Laser Part Beams, **22**, 275–278 (2004).
20. S. Dobosz, H. Stabile, A. Tortora, P. Monot, F. Reau, M. Bougeard, H. Merdji, B. Carre, Ph. Martin, D. Joyeux, D. Phalippou, F. Delmotte, J. Gautier, R. Mercier, Rev. Sci. Instrum. **80**, 113102 (2009)
21. S. Kazamias, F. Weihe, D. Douillet, C. Valentin, T. Planchon, S. Sebban, G. Grillon, F. Auge, D. Hulin, Ph. Balcou, Eur. Phys. J. D. **21**, 353 (2002)
22. N. Bloembergen, *Nonlinear Optics* (Benjamin, New York, 1965)
23. S.V. Fomichev, P. Berger, B. Carre, P. Agostini, D.F. Zaretsky, Laser Phys. **12**, 383–388 (2002)
24. J.B. Bertrand, H.J. Worner, H.C. Bandulet, E. Bisson, M. Spanner, J.C. Kieffer, D.M. Villeneuve, P.B. Corkum, Phys. Rev. Lett. **106**, 023001 (2011)
25. A. Ozawa, A. Vernaleken, W. Scheneider, I. Gotlibovych, Th. Udem, T.W. Hansch, Opt. Express **16**, 6233 (2008)
26. B. Zielbauer, D. Zimmer, J. Habib, O. Guilbaud, S. Kazamias, M. Pittman, D. Ros, Appl. Phys. B. **100**, 731–736 (2010)
27. http://www.nist.gov/pml/div685/grp07/al_detector.cfm
28. N.P. Delone, V.P. Krainov, Phys. Usp **41**, 469 (1998)
29. B. Cros, T. Mocek, I. Bettaibi, G. Vieux, M. Farinet, J. Dubau, S. Sebban, G. Maynard, Phys. Rev. A **73**, 033801 (2006)
30. V.J. Vlcek, Phys. D. **22**, 623 (1989)
31. M.G. Kapper, J.L. Cambier, J. Appl. Phys. **109**, 113308 (2011)
32. D.H. Reitze, S. Kazamias, F. Weihe, G. Mullot, D. Douillet, F. Aug, O. Albert, V. Ramanathan, J.P. Chambaret, D. Hulin, P. Balcou, Opt. Lett. **29**, 86–88 (2004)
33. S. Kazamias, S. Daboussi, O. Guilbaud, K. Cassou, D. Ros, B. Cros, G. Maynard, Phys. Rev. A. **83**, 063405 (2011)